Extreme Wind Gust Impact on UK Offshore Wind Turbines: Long-Term Return Level Estimation

Sara Abdelaziz, Sarah N. Sparrow, Weiqi Hua, David Wallom
Oxford e-Research Centre
University of Oxford
Oxford, UK
Sara.abdelaziz@eng.ox.ac.uk, sarah.sparrow@oerc.ox.ac.uk, weiqi.hua@eng.ox.ac.uk, david.wallom@oerc.ox.ac.uk

***Abstract*—Wind turbines (WT) are built to a particular standard based on past or current climate conditions. With climate change, the frequency of exposure of a WT to extreme weather events (EWE) will be more extreme than those for which they were designed, which may lead to decreasing operational performance and physical damage to the turbine structure. Given this, there is a need to investigate the location of future planned offshore wind farms (OWF) to ensure resilience to future wind extremes. The research presented covers the UK exclusive economic zone (EEZ) and uses the 2.2km UK Climate Projection 2018 (UKCP18) hourly maximum wind gust datasets. Two future scenarios corresponding to 2021-2040 and 2061-2080 are considered for future planning analysis. The statistical characterization of extreme wind gusts is assessed using multiple distributions, and a Beta distribution is found to adequately predict the hourly wind gust data. Changes in extreme wind loading on wind turbine structures (50-year return period, hereafter U_{50}) are investigated. Both risk ratio (RR) and relative change (RC) calculations have been used to set the recommended site from the achieved wind gust threshold corresponding to a U_{50}. As a result, regions in the North have a 99.6% increase in desired OWF siting locations in the 2061-2080 scenario. The East region has a 71.4% increase in the 2021-2040 scenario. In both scenarios, the South region has a decreased number of suitable future locations to site OWF.**

***Index Terms*-- Climate change, Extreme high wind gust, Offshore wind farms, Spatial planning.**

I. INTRODUCTION

Climate change is expected to alter the frequency and intensity of extreme weather events (EWE). This could impact wind energy generation in the UK and have further implications for reaching the net-zero carbon emissions target by 2050. Exposing wind turbines (WT) to EWE can lead to failure in WT structure [1] and acceleration in the wear of WT components which can also increase the fatigue load on the WT structure [2]. Therefore, future offshore wind farms (OWF) locations must be resilient to possible changes in future weather, given current WT design specifications. This research defines EWE based on the WT manufacturer threshold. The threshold represents the extreme load limit for the WT defined by a 50-year return period (U_{50}). By investigating the threshold in future wind scenario data, it is possible to quantify the effect that likely future wind extremes could have on WT operation in a specific location and thereby inform the optimal siting of future OWF in the UK. According to the International Electrotechnical Commission (IEC 61400-1) standard, U_{50} is a key determinant of WT structural loading due to extreme wind speed and is used to inform WT design in a specific area [3]. In an area prone to extreme wind speed, U_{50} is set high, which will increase the capital cost value. More accurate siting of WT leads to installation in locations less at risk from EWE and limits over-engineering of WT for a given deployment location, thereby potentially reducing financing costs for a specific project capital cost.

There is a wide range of location diversity in investigating extreme high wind speeds using historical models or observational data. For example, on the east coast of New Jersey, Debnath et al. [4] used the available observation data from floating lidars to assess extreme events, finding for 100m height wind speed that almost 100 events occur throughout the year. In Bangladesh [5], simulations of tropical cyclones produce exceedance probability estimates for extreme wind (gust). It has been found that Khulna, Barisal, and Chittagong provinces will experience maximum wind speed over cyclonic storm conditions > 25m/s, and areas within 30km of the coastline are predicted to experience gust speeds > 33m/s. Laurila et al. [6] studied extreme wind speed using the fifth-generation ECMWF atmospheric reanalysis wind dataset in North Atlantic and Europe from 1979 to 2018. The 98th percentile was used to define the extreme wind. The same research found a seasonal variation with the strongest winds over the ocean and during winter. Also, climate change models have been used in some regions such as North America [7] and Europe [8], [9] to investigate extreme wind speed events.

From the literature, we found a lack of in-depth spatial analysis for future changes in extreme wind gusts in the UK region, especially when coupled with WT manufacturer threshold. Consequently, in this research, the statistical characteristics will be evaluated spatially for the maximum wind gust in all offshore areas around the UK. We focus on

(Work was partially supported by the Schlumberger Foundation Faculty for the Future program)

climate change impacting future OWF sitation in four main regions covering the UK exclusive economic zone (EEZ) as we aim to analyze both the risk of future changes and exceedance in U_{50} manufacturer thresholds. The paper is organized as follows: Section II contains the climate model used, the region boundaries in the EEZ, and the wind turbine model. Section III contains the method to calculate U_{50}. Section IV presents the results of U_{50} relative change (RC) and the risk of exceeding U_{50} (risk ratio (RR)). Section V discusses the conclusions.

II. DATA PREPARATION

This section gives an overview of all data used in this research, including the maximum wind gust dataset, regions considered in EEZ, and the estimated wind turbine model.

A. Wind Gust

This research uses the surface maximum wind gust data, which is taken as the maximum value of 10 minutes in one hour. This wind gust data is taken from convection-permitting climate model projections (CPM) produced as part of the UK Climate Projection 2018 (UKCP18) project [10]. UKCP is a government-funded project that forms part of the Met Office Hadley Centre Climate Program [11]. The data is downscaled to a horizontal resolution of 2.2km. The high resolution provides an accurate estimation for mesoscale events, helping to inform adaptation to a changing climate [12]. The UKCP18 model simulation has 12 climate projections. Based on validating the offshore area in the UK against ERA5, we found the closest match in ensembles 01, 07, and 12. Due to computational constraints, this research uses ensemble 01. Three time periods are available in the data. The first is a baseline scenario (1981-2000), representing current climate conditions. Two future climate scenarios represent the near future (2021-2040) and the far future (2061-2080). Both future scenarios follow the Representative Concentration Pathway, RCP8.5, which refers to greenhouse gas emissions continuing to grow unmitigated, leading to a global average temperature rise estimation of 4.3°C by 2100, relative to pre-industrial levels [10].

B. The Regions of the UK Exclusive Economic Zone

Historically, shipping forecasts in the UK provide details of marine weather forecasts. Since 2002, the UK offshore areas have been divided into 31 shipping forecast areas [13]. Influenced by these areas, this research used the boundaries of the shipping forecast regions to define four major homogenous wind regions in the UK EEZ, East, South, West, and North (see TABLE II.I). The EEZ was adopted in 1982 at the third United Nations conference on the law of the sea. EEZ is an area of the sea in which a sovereign state has special rights regarding energy production from wind and water, and it is at a distance of 200 miles from the shore [14]. The regions are chosen based on merging multiple shipping forecast boundaries depending on their locations (East, South, West, and North). All four regions have been contoured with the EEZ mask. Internal boundaries representing the four regions are drawn on the map using black lines. TABLE II.I show the four offshore regions. The second column lists the latitude/ longitude box that fully encompasses each region. It should be noted that only available data in UKCP18 intersecting the EEZ have been considered in the analysis. The UKCP18 (2.2km) is only available in a latitudinal boundary equal to 60.58° N, which does not cover the north region of the EEZ (latitude boundary is 63.5° N) and so the results are truncated at 60.58° N. The third column has the region area, with the West region being the largest and the South region the smallest. The fourth column lists the shipping areas included and merged into each region. The paper analysis has been done in terms of a comparison between the four regions.

TABLE II.I. THE LOCATIONS OF THE FOUR REGIONS (EAST, SOUTH, WESTEST, AND NORTH).

Region	Location	Area (mile)	Included coastal sea areas
East	[-4.422°,51.226° : 3.399°,58.500°]	72426	Cromarty, Forth, Forties, Tyne, Dogger, Humber, Thames,
South	[-10.809°,47.435° : 1.932°,51.226°]	30923	Sole, Plymouth, Portland, Wight, Dover,
West	[-14.897°,49.998° : 2.628°,60.150°]	111055	Malin, Hebrides, IRIS sea, Lundy, Fastnet, Bailey, Rockall
North	[-8.470°,58.448° : 2.076°, 62.007°]	51136	Fair isle, Viking, Faeroes

C. Wind Turbine Model

The output capacity for newly built wind turbines is expected to reach 17MW and 151m hub height by 2035 [15]. We used this closest estimation for the turbine model. The wind gust data used in this research is scaled to 151m hub height using empirical relationships [16].

III. METHODS

This section tests the best-fitting distribution to wind gust data using nonparametric tests and introduces the U_{50} calculation in the context of future climate change.

A. Hourly Wind Gust Best Fit

Accurately estimating the frequency and magnitude of EWE is an essential part of energy development as it increases the stockholder's confidence in financial and risk analysis. Due to topographical and geographical differences, wind resources can vary from one location to another. Therefore, spatial assessment of EWE for the UK EEZ is necessary to site OWF accurately [17]. Using the baseline scenario, we use multiple probability density functions to assess wind gust variability and uncertainty; the main goal is to determine the best fit for the wind gust distribution. Four distributions have been used to spatially predict hourly wind gust statistics at a hub height of 151m. The distributions are Gamma [18], Beta [19], Exponential Weibull [20], and Generalized extreme value (GEV) [21]. The Kolmogorov-Smirnov (K-S) test and Cramér-von Mises [22] have been used to test the goodness of fit for all data. Both tests use the P-value to indicate that the wind gust data conforms with the given distribution. If the P-value is lower than a threshold of 0.01 (99% confidence interval), we reject the null hypothesis and conclude the data are not distributed according to the tested distribution. In

TABLE III.I, P-values are shown for baseline scenarios. The wide variety of shapes in beta distribution added flexibility to the distributions. The analysis reveals that the Beta distribution produces the highest P-value > 0.01 compared to the other three distributions, equal to 0.28 in the K-S test and 0.19 in the Cramér-von Mises test.

TABLE III.I. CRAMER-VON MISES AND K-S TESTS WERE APPLIED TO DISTRIBUTIONS USING THE 1891-2000 SCENARIO.

Tests	Gamma	GEV	Exponentiated Weibull	Beta
Cramér-von Mises test	$1.43*10^{-9}$	$6.02*10^{-9}$	$3.49*10^{-7}$	0.19
K-S test	$4.07*10^{-63}$	$7.62*10^{-74}$	0	0.28

B. *Calculate The 50-Year Return Period Considering Climate Change Signals.*

We investigated the extreme wind loading risk on WT structures using U_{50} [3]. The corresponding value for U_{50} has been calculated spatially using Beta distribution. The calculation has been done on the historical and the two future scenarios. In Fig 1, a single-cell grid is used to show the wind gust threshold (m/s) corresponding to the U_{50} (black arrow pointing toward the north).

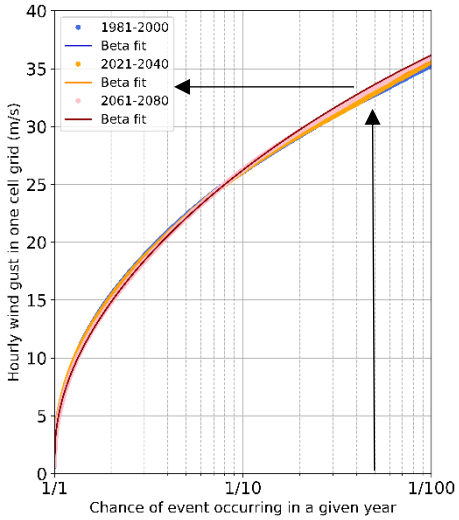

Figure 1. Return period for wind gusts using beta distribution in a single cell grid for the 1981-2000, 2021-2040, and 2061-2080 scenarios. The bold black lines refer to the U_{50} (x-axis) and the corresponding wind gust (y-axis).

In this research, we consider the changing magnitude of the U_{50} wind gusts event in the future (see Results, (*A*)), the RC of climate change signals is calculated as follows:

$$RC = ((V_j - V_i) / V_i) \quad (1)$$

Where RC is the relative change, V_j is the final value, and V_i is the initial value. In addition, we are looking at how the probability of exceeding the baseline thresholds changes (see Results, (*B*)). The RR has been calculated as follows:

$$RR = (H/total\_H)/(F/total\_F) \quad (2)$$

Where RR is the risk ratio. H and F are the numbers of wind gust data exceedance the U_{50} thresholds in the historical and future scenarios, respectively. $total\_H$ and $total\_F$ are the total numbers of data available in the historical and future scenarios, respectively.

IV. RESULTS

A. *Thresholds Corresponding To a 50-Year Return Period*

A Beta fit is applied spatially to the three scenarios to determine the return period. We investigated the extreme gust loading on wind turbine structures in two future scenarios by calculating the wind gust corresponding to U_{50} in the three scenarios, we calculate the future change compared to the baseline scenario. Fig 2 shows a statistical comparison between the four regions, East, South, West, and North. 2061-2080 has many locations with wind gusts equal to 36m/s compared to other scenarios. In the South region, the 2021-2040 scenario has a high probability of 35m/s wind gust and a high median value compared to the other two scenarios. Both the West and North regions show the U_{50} wind gust threshold will decrease in two future climate scenarios. East region has a lower probability of occurring U_{50} in the 2021-2040 scenario compared to the other two scenarios, implying less exposure of assets built in these areas to high wind gusts in the future.

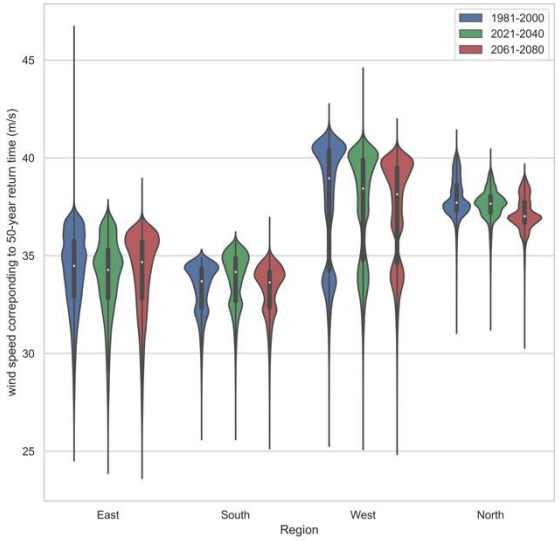

Figure 2. Violin plot for wind gust corresponding to U_{50}, and the results are in (m/s). The four panels are regions East, South, West, and North. (1981-2000 (blue), 2021-2040 (green), 2061-2080 (red)).

The RC calculation gave a good indication for increasing/ decreasing changes in two future scenarios. Three wind gust RC to U_{50} are shown in Fig 3 (a) 2021-2040 relative to 1981-2000, Fig 3 (b) 2061-2080 relative to 1981-2000, and Fig 3 (c) 2061-2080 relative to 2021-2040. In Fig 3, a positive relative difference indicates that the wind gust threshold corresponds to U_{50} has an increased risk in the future scenario compared to the baseline scenario (undesired site). At the same time, negative values show that the wind gust threshold in future scenarios is smaller than the baseline scenario, which indicates decreasing risk (desired site). Most locations in Fig 3 show marginal changes between scenarios. In 2021-2040 relative to 1981-2000, Fig 3 shows a desirable area for siting OWF in the

TABLE IV.I. REGION RECOMMENDATIONS.

	2021-2040 relative to 1981-2000				2061-2080 relative to 1981-2000				2061-2080 relative to 2021-2040			
	East	*South*	*West*	*North*	*East*	*South*	*West*	*North*	*East*	*South*	*West*	*North*
Increasing negative RC compared to positive RC	71.4%	-99.4%	52.8%	48.2%	28.6%	1.4%	36%	99.6%	30%	99.4%	38.8%	78.4%

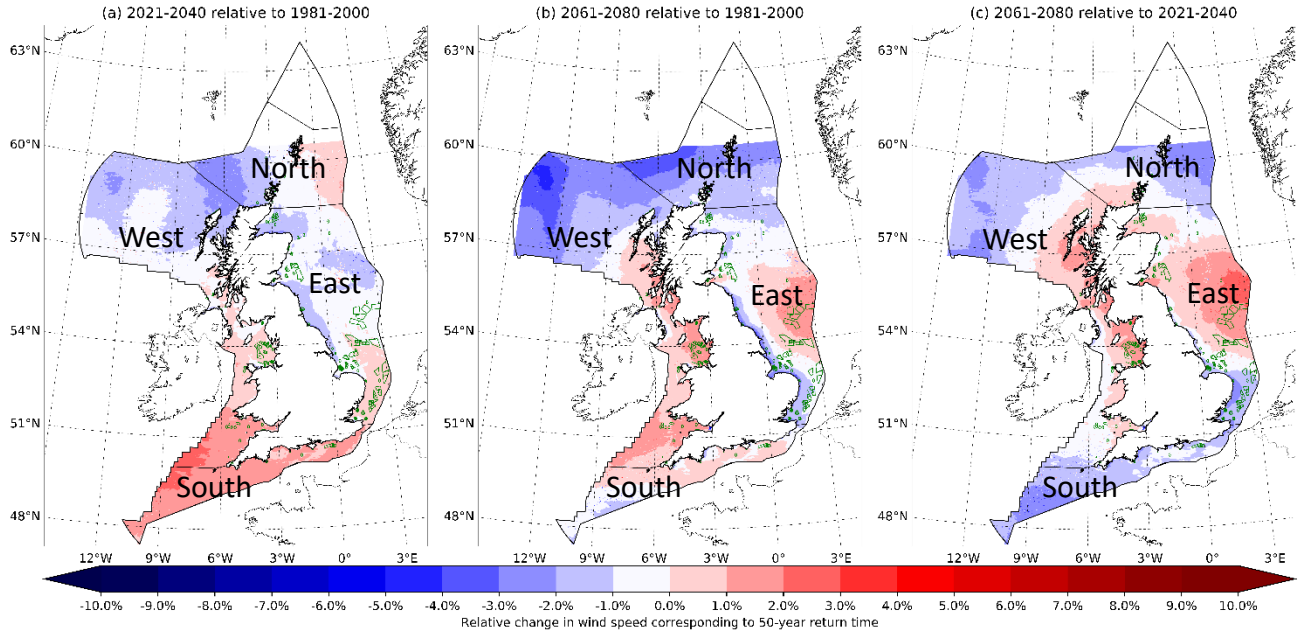

Figure 3. RC in wind gusts corresponds to U_{50}. (a) 2021-2040 relative to 1981-2000, (b) 2061-2080 relative to 1981-2000, and (c) 2061-2080 relative to 2021-2040. Black outer boundaries represent the EEZ, and black internal boundaries are the four regions. The green lines represent the UK Round 1, 2, 3, and 4, and the floating wind farms locations.

East region above latitude 54° N and in the north of the UK. 2061-2080 relative to 1981-2000 and 2061-2080 relative to 2021-2040 show more locations in the East region experiencing positive RC values. Most negative RC locations in 2061-2080 relative to 1981-2000 lay in the north of the West and North regions (above latitude 57° N), indicating a consistent trend to lower U_{50} values in these areas. In TABLE IV.I, the percentage of increasing the number of negative RC locations to positive RC locations for each region from Fig 3 is shown. The most suitable region will have a large percentage value. For 2021-2040 relative to 1981-2000, the East region is the most favorable, with 71.4% of the cell grid having decreased in the magnitude of U_{50} (increased in the number of desired siting locations in the future). The South is the worst, with 99.4% of locations experiencing an increase in the magnitude of U_{50} (decreased number of desired siting locations in the future). West and North regions have increased desired locations by 52.8% and 48.2%, respectively. In 2061-2080 relative to 1981-2000, the North region is the most desirable for siting OWF with 99.6%, and the South is the worse with a value equal to 1.4%. In 2061-2080 relative to 2021-2040, the North and South regions have the highest value, equivalent to 78.4% and 99.4%, respectively. At the same time, the East and West regions have the smallest values, equal to 30% and 38.8%, respectively.

B. Risk Ratio Calculation

We are taking the U_{50} threshold from the baseline and working out the probability of meeting or exceeding that threshold in future scenarios. RR = 1 means that exceeding a certain threshold does not affect the specific scenario. RR < 1 means that the risk of exceedance of a certain threshold is increased in the future scenario. RR > 1 means that exceeding a certain threshold has become less common in this future scenario. Fig 4 shows the RR between historical scenario thresholds and 2021-2040 (blue) and 2061-2080 (green). Higher RR values mean lower exceeding risk in the scenario. In 2021-2040, there is a pronounced increase in exceedance risk in the South region, with a median equal to 0.86, compared to the other three regions. In 2061-2080, the West region has the highest range of RR; a reason can be that it has the most significant area compared to other regions, see TABLE II.I. The north of the West region has a decreasing exceeding risk which explains the long tail toward values of RR > 1 in the plot. In the same scenario, the exceeding risk decreases in the North region with a median equal to 1.22, giving the best result compared to other regions. The RR results conform with the RC results. In 2061-2080, the North region has the highest recommended siting locations. In 2021-2040, most locations in the North and East regions have RR > 1. The South region has the least favorable sites for future OWF installation.

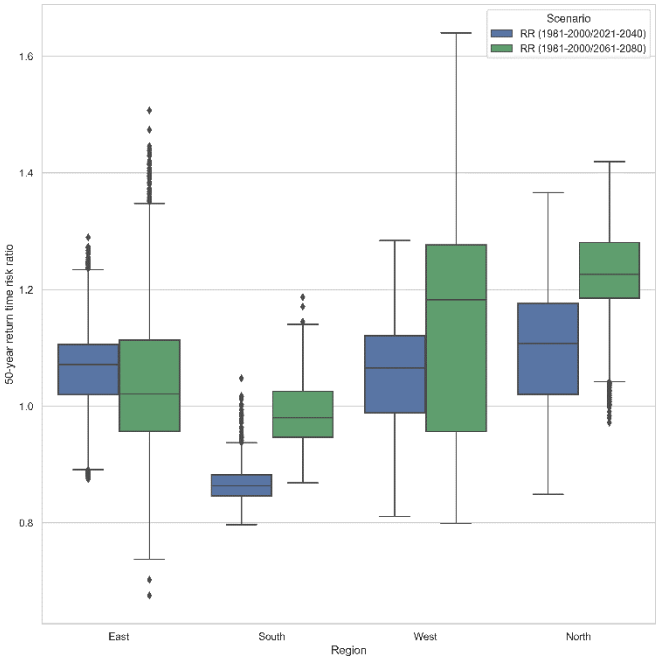

Figure 4. Box plot for RR of wind gust (m/s) corresponding to U_{50}. The four panels are regions East, South, West, and North. (RR between 2021-2040 and 1981-2000 (blue), RR between 2061-2080 and 1981-2000 (green).

V. CONCLUSION

Mitigating possible future weather risks that OWF will be exposed to can lead to longer wind turbine lifetime and sustained investment in wind energy. In this research, we investigate the future change in climate change signals using the wind turbine manufacturer threshold for extreme loading. Analysis showed that Beta distribution most closely represents the hourly wind gust data within UK EEZ. We have demonstrated the RC in U_{50} over the four regions between the three different time points. RC in U_{50} has been used to establish recommended sites for future OWF installation. The East and North regions showed the most favorable indicators to install future OWF in 2021-2040, equal to 71.4% and 48.2% increase in desired future locations, respectively. For 2061-2080, the North region has the most significant increase in desired future installations, equivalent to 99.6%. The South is the least favorable in both future scenarios. Exceeding the U_{50} is considered by using RR calculations. The RR results conform with RC calculations for recommended OWF siting. Most RR > 1 in 2021-2040 lay in the North and East region. In 2061-2080, The dominant RR > 1 lay in the North region.

ACKNOWLEDGMENT

The authors would like to acknowledge the use of the University of Oxford Advanced Research Computing (ARC) http://dx.doi.org/10.5281/zenodo.22558.

REFERENCES

[1] A. G. Olabi *et al.*, "A review on failure modes of wind turbine components," *Energies*, vol. 14, no. 17, 2021, doi: 10.3390/en14175241.

[2] L. Dueñas-Osorio and B. Basu, "Unavailability of wind turbines due to wind-induced accelerations," *Eng. Struct.*, vol. 30, no. 4, pp. 885–893, 2008, doi: 10.1016/j.engstruct.2007.05.015.

[3] P. D. I. E. C. Ts, "BSI Standards Publication Wind energy generation systems," 2019.

[4] M. Debnath, P. Doubrawa, M. Optis, P. Hawbecker, and N. Bodini, "Extreme wind shear events in US offshore wind energy areas and the role of induced stratification," *Wind Energy Sci.*, vol. 6, no. 4, pp. 1043–1059, 2021, doi: 10.5194/wes-6-1043-2021.

[5] H. Steptoe and T. Economou, "Extreme wind return periods from tropical cyclones in Bangladesh: Insights from a high-resolution convection-permitting numerical model," *Nat. Hazards Earth Syst. Sci.*, vol. 21, no. 4, pp. 1313–1322, 2021, doi: 10.5194/nhess-21-1313-2021.

[6] T. K. Laurila, V. A. Sinclair, and H. Gregow, "Climatology, variability, and trends in near-surface wind speeds over the North Atlantic and Europe during 1979–2018 based on ERA5," *Int. J. Climatol.*, vol. 41, no. 4, pp. 2253–2278, 2021, doi: 10.1002/joc.6957.

[7] D. Il Jeong and L. Sushama, "Projected changes to mean and extreme surface wind speeds for North America based on regional climate model simulations," *Atmosphere (Basel).*, vol. 10, no. 9, 2019, doi: 10.3390/atmos10090497.

[8] S. Outten and S. Sobolowski, "Extreme wind projections over Europe from the Euro-CORDEX regional climate models," *Weather Clim. Extrem.*, vol. 33, p. 100363, 2021, doi: 10.1016/j.wace.2021.100363.

[9] S. C. Pryor, R. J. Barthelmie, N. E. Clausen, M. Drews, N. MacKellar, and E. Kjellström, "Analyses of possible changes in intense and extreme wind speeds over northern Europe under climate change scenarios," *Clim. Dyn.*, vol. 38, no. 1–2, pp. 189–208, 2012, doi: 10.1007/s00382-010-0955-3.

[10] D. Konneh, H. Howlader, R. Shigenobu, T. Senjyu, S. Chakraborty, and N. Krishna, "A Multi-Criteria Decision Maker for Grid-Connected Hybrid Renewable Energy Systems Selection Using Multi-Objective Particle Swarm Optimization," 2019. doi: 10.3390/su11041188.

[11] CEDA, "UK Climate Projections 2018 (UKCP18)." https://catalogue.ceda.ac.uk/uuid/c700e47ca45d4c43b213fe879863d589?_ga=2.164002815.1334446900.1624300753-1212288270.1616941503 (accessed Jun. 22, 2021).

[12] E. J. Kendon *et al.*, "UKCP Convection-permitting model projections: Science report," 2019.

[13] N. M. Library, "Fact sheet 8 — The Shipping Forecast National Meteorological Library and Archive."

[14] MMO, "United Kingdom commercial sea fisheries landings by Exclusive Economic Zone of Capture," 2017. [Online]. Available: https://www.gov.uk/government/uploads/system/uploads/attachment_data/file/647579/United_Kingdom_commercial_sea_fisheries_landings_by_Exclusive_Economic_Zone_of_capture_2012_.pdf.

[15] R. Wiser *et al.*, "Expert elicitation survey predicts 37% to 49% declines in wind energy costs by 2050," *Nat. Energy*, p. 14, 2020, [Online]. Available: http://dx.doi.org/10.1038/s41560-021-00810-z.

[16] S. Grassi *et al.*, "Mapping of the global wind energy potential using open source GIS data," *2nd Int. Conf. Energy Environ. bringing together Eng. Econ.*, no. June, p. 6, 2015.

[17] F. P. Bakker, "Characterisation of the South African Extreme Wind Environment Relevant to Standardisation by," 2021.

[18] T. A. BURGIN., "The Gamma Distribution and Inventory Control," *Oper. Res. Q.*, vol. 28, no. 3, pp. 663–670, 1975.

[19] M. Nedaei, E. Assareh, and P. R. Walsh, "A comprehensive evaluation of the wind resource characteristics to investigate the short term penetration of regional wind power based on different probability statistical methods," *Renew. Energy*, vol. 128, no. 2018, pp. 362–374, 2020, doi: 10.1016/j.renene.2018.05.077.

[20] R. Barrios and F. Dios, "Exponentiated Weibull distribution family under aperture averaging for Gaussian beam waves," *Opt. Express*, vol. 20, no. 12, pp. 1735–1740, 2012.

[21] A. J. R. M. Hosking, J. R. Wallis, and E. F. Wood, "Estimation of the Generalized Extreme- Value Distribution by the Method of Probability-Weighted Moments," *Taylor Fr.*, vol. 27, no. 3, pp. 251–261, 1985.

[22] V. K. R. A. . K. M. E. Saleh, *An Introduction to Probability and Statistics*, Second. WILEY, 2000.